Interstitial migration in irradiated iron and iron-based dilute alloys. II. Interstitial migration and solute transport in FeNi, FeMn and FeCu dilute alloys

1990 J. Phys.: Condens. Matter 2 9291

(http://iopscience.iop.org/0953-8984/2/47/005)

J. Phys.: Condens. Matter 2 (1990) 9291–9307. Printed in the UK

Interstitial migration in irradiated iron and iron-based dilute alloys: II. Interstitial migration and solute transport in FeNi, FeMn and FeCu dilute alloys

F Maury†, A Lucasson, P Lucasson, P Moser‡ and F Faudot§
UA CNRS No 803, Université Paris XI, F-91405 Orsay, France

Received 17 July 1989, in final form 2 July 1990

Abstract. Three series of dilute iron alloys, **Fe**Ni, **Fe**Mn and **Fe**Cu, with concentrations ranging from 50 at.ppm to 3 at.%, have been electron-irradiated at low temperature and annealed up to room temperature. The recovery spectra of the radiation-induced resistivity show that mixed-interstitial migration takes place, in the **Fe**Ni alloys, at the beginning of stage II (130–150 K, depending on the Ni concentration), thus providing evidence of the formation of stable mixed-interstitial Fe–Ni during self-interstitial migration in stage I. Mixed interstitials are deduced to be formed also in **Fe**Mn and **Fe**Cu alloys although they are not stable above stage I and are not directly observable.

Mixed poly-interstitials migrate below stage III (i.e. below 200 K) in the three alloys studied. Such a migration instead of break-up results in the growth of larger mixed-interstitial clusters and leads to solute clustering and correlated solute bulk depletion. Bulk depletion was indeed observable in the **Fe**Cu and, to a lesser extent, in the **Fe**Ni dilute alloys through a diminution of the residual resistivity of the samples. In the **Fe**Mn concentrated alloys (1 and 3%), the mixed poly-interstitial clustering gives rise in stage II to γ-precipitation which largely survives the vacancy migration.

1. Introduction

It is well known that copper at concentrations $\geqslant 0.1\%$ is responsible for important radiation embrittlement in low alloy ferritic steels. The presence of nickel at levels $\leqslant 1\%$ augments the primary embrittlement due to copper; at higher concentrations, nickel induces a significant embrittlement even in low copper ($\leqslant 0.1\%$) alloys. Among other impurity or alloying elements that play either a secondary or a negligible role in radiation-enhanced embrittlement (see Little 1984 and references therein) we chose manganese, which is the main alloying element in current pressure vessel steels (at typical concentrations of 1 to 1.5%).

Like Co and Cr and unlike Mo, Ti and V, the two solutes Ni and Mn have a negligible or small ($<5\%$) size effect in Fe (King 1966). If we look at a more local parameter than the volume size factor, like the Goldschmidt or Seitz atomic radius, copper (whose volume size factor is $+17.5\%$), is found of the same size as Fe and Cr. The present work

† Present address: Laboratoire des Solides Irradiés, Ecole Polytechnique, F-91128 Palaiseau Cédex, France.
‡ CEN G-DRF-SPh MP, 85 X, F-38041 Grenoble Cédex, France.
§ CECM, 15 rue G Urbain, F-94407 Vitry, France.

0953-8984/90/479291 + 17 $03.50

shows that bound mixed interstitials are indeed formed in these three alloys: **Fe**Ni (section 3); **Fe**Mn (section 4), and **Fe**Cu (section 5). By mixed interstitial, we mean an interstitial configuration where the substitutional solute atom has been pushed out of its lattice site and has replaced one of the two Fe atoms of the split self-interstitial, whatever the final configuration may be (⟨110⟩ dumbbell or not).

2. Specimens' characteristics

The experimental conditions (sample elaboration, irradiation and measurements) were described in paper I (Maury *et al* 1990). Table 1, below, shows the specimens' characteristics for the three alloys **Fe**Ni, **Fe**Mn and **Fe**Cu. For the **Fe**Cu samples No 2.1 to 2.6, no separate potential leads were mounted onto the samples. Thus only an upper limit could be determined for the shape factor and consequently for the radiation-induced resistivity, $\Delta\rho_0$. Besides, no unalloyed iron was available, impeding furthermore the determination of the apparent solute specific resistivity, $\rho_s = [\rho_{4K}(\text{alloy}) - \rho_{4K}(\text{Fe})]/c_s$.

Two different sets of **Fe**Ni alloys were prepared; the first one (irradiated in run 6) was elaborated and annealed (4 h at 730 °C) in Grenoble; the second one (irradiated in run 8) was elaborated and annealed (24 h at 850 °C) in Vitry. They differ in their residual resistivity. Note that the residual resistivity of two other Fe + 1% Ni samples, prepared in Vitry and which have not been irradiated, was found equal to 1770 ± 10 nΩ cm, showing no scattering among the Vitry samples.

The observed deviations from Matthiessen's rule are discussed in paper I (section 3).

3. Mixed-interstitial formation and migration in FeNi alloys

3.1. Stage I recovery

Figure 1 shows the recovery spectra of Fe and **Fe**Ni samples irradiated in run 6 plus two **Fe**Ni samples irradiated in run 8. Since α_{Ni} is greater than 1, the resistivity data do not require much correction for deviations from Matthiessen's rule (see paper I).

As observed previously (Blythe *et al* 1984, Maury *et al* 1986), increasing concentrations of nickel gradually suppress the stage I_E recovery. Figure 1 shows that stage I_E around 130 K, which can be attributed to self-interstitial long-range migration, is suppressed by 100 ppm Ni, the recovery around 115–120 K by 1000 ppm Ni. In contrast to the Mo case, no suppression of the I_{D1} and I_{D2} peaks (around 101 and 108 K) is observed on the measured spectra of the 1000 ppm alloy. In the same way, 1% Ni reduces these two peaks much less than does 1% Mo. This smaller reduction of the close pair recovery indicates that (i) the capture radius of a Ni atom is smaller than that of a Mo atom and/or that (ii) the resulting complex has a smaller extra-resistivity in the case of Ni than in the case of Mo. These two points are consistent with the assumption that a mixed-interstitial Fe–Ni forms during the self-interstitial migration in **Fe**Ni alloys (Maury *et al* 1986).

Surprisingly, the present data show that the low-temperature recovery is enhanced in the 3% alloy, as compared to the metal, by about 20%. Table 2 gives the percentages of the extra-resistivity retained at 94 K in the metal and in the alloys Fe + 1% Ni, Fe + 3% Ni together with Fe + 1% Mo and Fe + 3% Mo for comparison.

Table 1. Specimens' characteristics.

Alloy	Sample number†	Sample mean thickness (μm)	Solute concentration, c_s	Residual resistivity, $\rho_0 \equiv \rho_{4K}$ (nΩ cm)	Apparent solute specific resistivity, ρ_s^* ($\mu\Omega$ cm)	Solute specific resistivity from literature ($\mu\Omega$ cm)	Irradiation conditions		Radiation-induced resistivity, $\Delta\rho_0$ (nΩ cm)
							Dose (e^- cm $^{-2}$)	Temperature (K)	
FeCu	1.1	$\simeq$27	0	33	—		6.3×10^{17}	20	62–58–59
	1.2	$\simeq$15	4×10^{-4}	132	250			21	79–71–70
FeCu	2.1	30 ± 2	5×10^{-5}	>62					
	2.4	35 ± 3	5×10^{-5}	>60			6.3×10^{17}	19	>46
	2.2	36 ± 1	10^{-4}	>75				20	>50
	2.5	36 ± 2	10^{-4}	>73				20	>51
	2.3	37 ± 2	2×10^{-4}	>88				21	>55
	2.6	29 ± 2	2×10^{-4}	>82				24	>55
								20	>57
FeMn	5.2	59	0	58	—		7.4×10^{17}	37	59
	5.3	49 ± 1	10^{-4}	117	600	170–175[a]		40	67
	5.4	48 ± 1	10^{-3}	480	420	140[b]		35	82
	5.1	47 ± 1	10^{-2}	1800	175	170[c]		35	180
	5.5	45 ± 2	10^{-2}	1900	185	130[d]		34	180
	5.6	55	3×10^{-2}	3200	105			38	270
FeNi	6.6	57	0	60	—		7.4×10^{17}	34	56
	6.2	61	10^{-4}	80	230	200[a]		35	60
	6.3	52	10^{-3}	290	230	190[b]		33	76
	6.1	53 ± 2	10^{-2}	2200	220	180[c]		34	100
	6.4	50	10^{-2}	2250	220	210[d]		34	100
	6.5	47	3×10^{-2}	5800	190			33	110
FeNi	8.3	48	0	34	—		7.4×10^{17}	22	55
	8.2	50	10^{-2}	1850	180			28	120
	8.1	50 ± 1	3×10^{-2}	5150	170			25	120

† The first figure is the experiment number, the second one refers to the position of the sample on the sample holder.
[a] Campbell *et al* (1967) [b] Arajs *et al* (1969) [c] Fert and Campbell (1975) [d] Dorleijn and Miedema (1976)

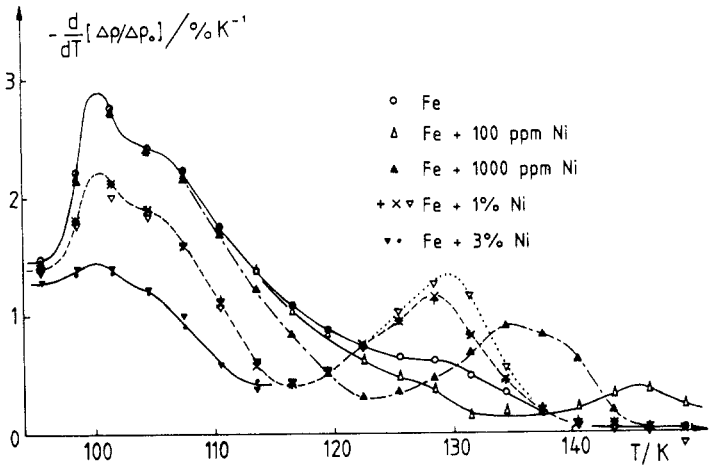

Figure 1. Differentiated isochronal recovery spectra of Fe and **Fe**Ni alloys: Samples No 6.6 (○), 6.2 (△), 6.3 (▲), 6.1 (×), 6.4 (+), 6.5 (●), 8.2 (▽) and 8.1 (▼). $\Delta t = 300$ s.

Table 2. Percentage of the radiation-induced resistivity retained at 94 K: $100\,\Delta\rho(94\text{ K})/\Delta\rho_0$.

Alloy	Fe (8 samples)	Fe + 1% Ni	Fe + 3% Ni	Fe + 1% Mo	Fe + 3% Mo
Without correction	68.5–71.8	66.8, 67.0, 69.4	58.5, 57.9	72.7	75.1
After ρ_F^* correction	65–66	66, 66, 68.5	58, 57.5	71	74.5

The increase usually observed in $\Delta\rho(94\text{ K})/\Delta\rho_0$ at solute concentrations of a few per cent is readily explainable as the consequence of the reduction of close pair recombination: the self-interstitials become trapped before they can reach their correlated vacancy or even during the creation process itself. If one neglects this creation of directly trapped interstitials, an enhancement of the resistivity recovery in the close pair recovery region is hardly understandable even if the capture of self-interstitials by solute atoms results in a loss of extra-resistivity. On the other hand, it can be understood if, for example, some close pairs which would not have been stable in Fe are stabilized by the presence of the Ni atoms. It could also happen that self-interstitials created in regions containing more than one Ni atom induce small γ-precipitates: the solubility of Ni in Fe is strongly reduced when the pressure is increased (Kaufman and Ringwood 1961). In these non-magnetic FCC precipitates, the self-interstitials could migrate between the irradiation temperature ($\leqslant$35 K) and 94 K.

3.2. Stage II recovery

3.2.1. Stage II_{Ni}. The results of the present experiment with more concentrated alloys are similar to those obtained previously (Maury *et al* 1986) with very dilute alloys. A recovery peak, which we label II_{Ni}, is observed at the beginning of stage II in the **Fe**Ni alloys; its amplitude is an increasing function of the Ni content of the alloy and its position

shifts from ≃150 K for the very dilute alloys to ≃130 K for the 1% alloy (cf figure 1). Such a shift is a clear indication of mixed-interstitial migration; it results from the fact that the initial correlation between interstitials and vacancies is partly preserved by the trapping process; it is preserved more the higher the trap concentration. (For a more detailed discussion see Maury *et al* (1988).)

The structure of a recovery stage arising from mixed-interstitial migration somewhat reproduces (*a*) the structure of the metal stage I if the migrating mixed interstitials are not retrapped by the solute atoms or (*b*) the structure of the alloy stage I if solute dumbbells or 'solute + mixed interstitial' complexes are formed. The fact that stage II_{Ni} is much larger in Fe + 1% Ni than in Fe + 100 ppm Ni shows that the mixed interstitials Fe–Ni are not retrapped by the Ni atoms. This is confirmed by the fact that the radiation-induced resistivity retained at the end of stage II_{Ni}, $\Delta\rho(157\text{ K})/\Delta\rho_0$, is the same in the alloy Fe + 1000 ppm Ni (12.3%) as in Fe (12.7 ± 0.9%) or Fe + 100 ppm Ni (13.0%). We are then in case (*a*) and the structure of stage II_{Ni}, which is clearly observable in the three alloys Fe + 1% Ni, Fe + 1000 ppm Ni and Fe + 100 ppm Ni, must reflect the successive annihilations of close pairs, correlated pairs and uncorrelated pairs 'mixed interstitial + vacancy'.

Let us note that peak II_{Ni} cannot be attributed to a conversion of trapped interstitials into more stable mixed interstitials as proposed by Blythe *et al* (1984) from magnetic relaxation measurements: a conversion process should not depend on the Ni concentration.

The mixed interstitials which are not annihilated at vacancies during their migration in stage II_{Ni} combine to form small mixed clusters or become trapped at residual impurities. The fact that the fractional resistivity retained at the end of stage II_{Ni} (157 K) is the same in the dilute alloys (13.0 and 12.3% for 100 and 1000 ppm Ni) and in the metal (12.7 ± 0.9%) is not incompatible with a specific resistivity retained per mixed interstitial Fe–Ni lower than that retained per self-interstitial Fe–Fe: apart from the big influence of the residual impurities, the difference could be counterbalanced by an enhanced formation of small poly-interstitials in the alloy as compared with the metal.

3.2.2. Stage II'_{Ni}. A second Ni-dependent recovery substage, II'_{Ni}, is observed at the end of stage II (see figure 2), which shows the same characteristics, although less marked, as II_{Ni}: its amplitude increases and its position shifts towards the low temperatures as the Ni concentration augments. We attribute this substage to the migration of the mixed poly-interstitials formed in II_{Ni}. The magnetic relaxation measurements of Vigier and Moser (1966) and Blythe *et al* (1982) have shown that the presence of nickel gives rise to a series of relaxation peaks which transform one into the other: one appears while another one disappears. Each of these peaks can be attributed to a given type of mixed poly-interstitial, the first peak around 80 K being attributed to the mixed single interstitial Fe–Ni; the successive growth and decay of these relaxation peaks reflect the progressive clustering of mixed poly-interstitials, which become mobile at increasing temperatures as their size augments.

This mixed-interstitial clustering leads to nickel gathering into Ni-rich small interstitial clusters and to correlated nickel bulk depletion which may, at least partly, survive the subsequent vacancy migration and interstitial annihilation in stage III. Solute bulk depletion has indeed been observed in Fe + 400 ppm Ni, electron-irradiated at 5 K and annealed at 300 K (Börner *et al* 1987), and was assumed to stem from an interstitial diffusion of the Ni atoms (Robrock 1987). Bulk depletion is also observable through

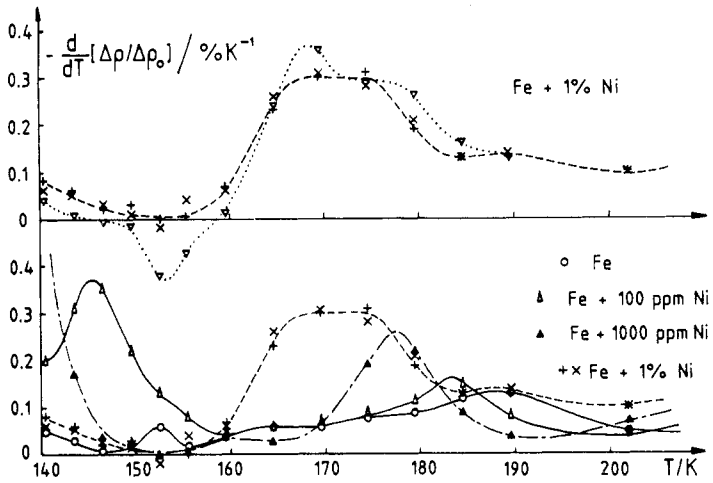

Figure 2. Same as figure 1.

resistivity measurements: the residual resistivity of dilute **FeNi** alloys is found to be smaller after irradiation at low temperature followed by several days at room temperature than it was before the irradiation; the loss in residual resistivity is the larger the higher the Ni content: for samples containing 50, 100, 200 and 400 ppm Ni, of initial resistivities $\rho_0 = 38.3, 51.7, 64.1$ and 110.1 nΩ cm, irradiated in a previous study (Maury *et al* 1986) with 17×10^{17} e$^-$ cm^{-2} at a temperature below stage II_{Ni} and annealed for 5 days at room temperature, the radiation-induced resistivity retained at 300 K, $\Delta\rho$ (300 K), was found equal to +0.7, +0.05, −0.10 and −0.55 nΩ cm respectively. This effect was reproducible: $\Delta\rho$ (300 K) was found to be negative for 200 and 400 ppm Ni in the three other runs performed below 120 K.

Now it is not *a priori* excluded that vacancy migration also contributes to solute agglomeration in addition to (or even more than) interstitial clustering. Vacancy-free migration takes place between 200 and 300 K; it gives rise, in pure Fe, to a resistivity recovery peak centred around 240 K (see figure 3 of paper I); in Fe + 1000 ppm Ni, this peak is replaced by two peaks centred around 210 and 260 K. The two following points support an interstitial rather than a vacancy mechanism for Ni agglomeration in these low-temperature irradiated dilute alloys.

(i) The vacancy concentration at the beginning of stage III was about 10 ppm in our experiments. Ni transport via a vacancy mechanism should have a high efficiency to account for a 0.5% loss of residual resistivity in Fe + 400 ppm Ni.

(ii) When the irradiation temperature was increased above stage II_{Ni}, $\Delta\rho$(300 K) was no longer found to be negative but became positive: $\Delta\rho$(300 K) was found equal to +1.65, +1.05, +0.6 and +0.5 nΩ cm in the above samples, containing respectively 50, 100, 200 and 400 ppm Ni, irradiated with 38×10^{17} e$^-$ cm^{-2} around 170 K and annealed for 3 days at room temperature. At this irradiation temperature where the mixed interstitials Fe–Ni are mobile, their instantaneous concentration is small so that the interstitial clusters are rather nucleated on heterogeneous defects; they are fewer in number, larger in size. As a consequence their stability is higher and they survive annealing at 300 K better, which augments $\Delta\rho$(300 K). But at the same time the vacancy

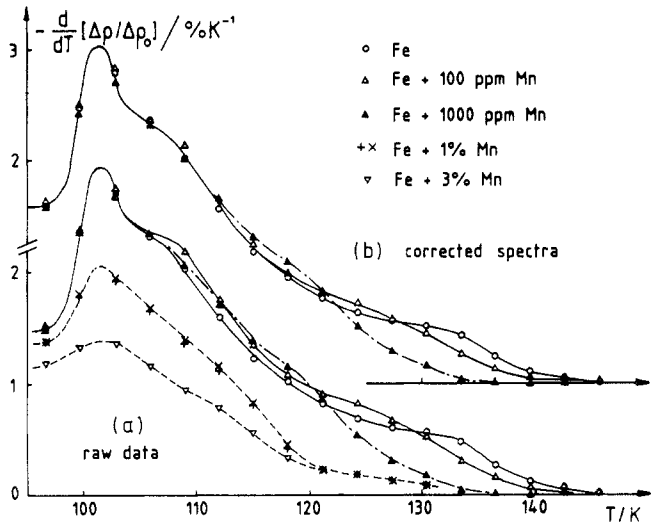

Figure 3. Differentiated isochronal recovery spectra of Fe and **Fe**Mn alloys. $\Delta t = 300$ s: (*a*) raw data, (*b*) after ρ_F^* correction. The correction is negligible for the 1% and 3% alloys.

migration path to these clusters is increased. This should facilitate the Ni clustering if the vacancy mechanism was dominant, and decrease $\Delta\rho(300\text{ K})$. Now $\Delta\rho(300\text{ K})$ is observed to increase showing no sign of a dominating vacancy mechanism for Ni agglomeration.

Let us turn finally to the alloys in the per cent range. For these alloys, the fraction of radiation-induced resistivity retained at the end of stage II_{Ni}, $\Delta\rho(157\text{ K})/\Delta\rho_0$, is no longer equal to that in the metal and dilute alloys. It becomes larger: 19.2 to 22.5% for 1 to 3% Ni instead of 11.7 to 13% for 0, 100 or 1000 ppm Ni. This augmentation can be attributed to multiple trapping. A new peak appears on the left side of substage II'_{Ni} (figure 2) which can stem from those multi-trapped interstitials. In the 3% alloy spectra (not shown in figure 2), multiple trapping levels the recovery in the whole stage II range (140–190 K).

Finally, in one of the Fe + 1% Ni alloys, an increase in the residual resistivity was observed around 155 K (figure 2). We interpret this as the result of a transformation to the γ-phase induced by the migration of Fe–Ni mixed interstitials in regions containing a sufficient number of Ni atoms. A similar effect of much larger amplitude is observed in the **Fe**Mn alloys.

4. Mixed-interstitial formation and migration in FeMn alloys

4.1. Stage I recovery

Figure 3(*a*) shows the measured resisitivity recovery spectra of Fe and **Fe**Mn samples irradiated in run No 5. One can see that the end of stage I is suppressed by manganese but significantly less than by nickel; the fractional radiation-induced resistivity retained at the end of stage I, $\Delta\rho(142\text{ K})/\Delta\rho_0$, is much smaller in the **Fe**Mn dilute alloys than in the **Fe**Ni alloys: $\Delta\rho(142\text{ K})/\Delta\rho_0 = 13.6$, 11.5 and 17.0% for 0, 100 and 1000 ppm Mn as

Table 3. Stage I recovery data for FeMn dilute alloys.

Alloy	α_0	$\Delta\rho_0$ (nΩ cm)	T_{irr} (K)	$\Delta\rho(94\text{ K})/\Delta\rho_0$ (%)	$\Delta\rho(142\text{ K})/\Delta\rho_0$ (%)
Uncorrected data					
Fe	—	59	36	69.7	13.6
100 ppm Mn	—	67	39	69.4	11.5
1000 ppm Mn	—	82	34	69.5	17.0
Corrected data					
Fe	2.5	45	36	67.2	11.6
100 ppm Mn	2.0	51	39	65.7	9.5
1000 ppm Mn	1.5	42.5	34	67.2	15.5

compared with 12.1, 18.0 and 24.4% for 0, 100 and 1000 ppm Ni, respectively. In particular the resistivity retained in the 100 ppm Mn alloy is not larger than in the metal. If we go back to figure 3(*a*), we see that the reduction at the end of stage I_E is balanced by an enhancement in the 110–130 K region. This enhancement is small and the difference between the metal and the 100 ppm alloy is not larger than that observed between two Fe samples (figure 2 of paper I). The two spectra can effectively be brought together up to 130 K by ρ_F^* correction with $\alpha_0(\text{Fe}) = 2.5$ and $\alpha_0(\text{Fe} + 100\text{ ppm Mn}) = 1.5$ (where α_0 is the α-parameter of the sample prior to the irradiation); but then the fractional recovery below 94 K, due to close pair recombination, becomes larger in the 100 ppm alloy than in the metal: $\Delta\rho(94\text{ K})/\Delta\rho_0 = 64.2\%$ in the alloy instead of 67.2% in the metal, indicating that the ρ_F^* effect has been slightly overestimated. The Fe + 1000 ppm Mn spectrum is only slightly modified by the correction. In any case it remains above the Fe spectrum in the temperature range 112–122 K. The corrected spectra of figure 3(*b*) have been obtained with the values of α_0 listed in table 3.

The variations of $\Delta\rho_0$ after ρ_F^* correction, which are correlated with the variations in the irradiation temperature from one sample to the other, reflect the inhomogeneity of the electron beam.

The enhancement of the recovery between 110 and 120 K in dilute FeMn alloys has already been observed in a previous experiment (Maury *et al* 1986). As in the present experiment, the fractional resistivity retained at the end of stage I was found to be the same, within the experimental uncertainties, in the metal and in the alloys up to 400 ppm Mn. This indicates that the Mn substitutional atoms do not retain the migrating interstitials above stage I_E (140 K). The weak influence of a low concentration of manganese on the stage I recovery of Frenkel defects is also demonstrated by the magnetic relaxation results of Vigier (1966), who has observed that 0.1% Mn does not modify significantly the magnetic after-effect measured between 100 and 200 K.

The enhancement of the recovery at the beginning of the free interstitial migration can stem from one or both of the two following causes.

(i) Mixed interstitials Fe–Mn are formed during self-interstitial migration, this occurs earlier with higher Mn concentration. They are more mobile than the self-interstitials and annihilate as soon as they have been formed.

(ii) Mixed interstitials Fe–Mn are formed with a specific resistivity less than the sum $\rho_s^* + \rho_i^*$, where ρ_s^* and ρ_i^* are the specific resistivities of Mn substitutional atoms and Fe self-interstitials in the alloy. The Fe–Mn mixed interstitials are mobile in stage I so

that the corresponding resistivity recovers in two steps: the first part recovers when the Fe–Mn interstitials are formed, the second when they are annihilated at vacancies.

In both cases the present interpretation implies that no single interstitial (self-interstitial Fe–Fe, mixed interstitial Fe–Mn or hetero-interstitial Mn–Mn) survive above stage I. Only mixed di-interstitials will be left at 140 K.

However, if we turn to the per cent alloys, we observe (figure 3) an important reduction of the I_D peaks, comparable with that observed in **Fe**V or **Fe**Ni alloys. Now the mixed interstitials Fe–Ni or the self-interstitials trapped at V atoms are stable and not mobile at the temperature of the I_D peaks, whilst in **Fe**Cr alloys, where mixed interstitials are migrating in stage I (Maury *et al* 1987), the I_D peaks are but slightly modified by 1% Cr. Then a question arises: are mixed interstitials Fe–Mn, or self-interstitials trapped at Mn atoms, stable at the temperature of the I_D peaks and up to stage II, contrary to the assumption above, or otherwise by what means are they retained in Fe + 1% Mn?

Let us recall that a qualitative difference between 0.1% and 1% Mn alloys has also been reported by Vigier (1966). But if we now turn to multiple trapping, its incidence should be comparable in **Fe**Mn and **Fe**V, i.e. not much (see paper I): in **Fe**Mn (Pierron and Cadeville 1982), like in **Fe**V, the interactions between solute atoms in first- or second-nearest-neighbour positions are found to be repulsive. There is a significant difference, however, between **Fe**Mn and **Fe**V alloys: in **Fe**Mn alloys the α-phase is much less stable than in **Fe**V alloys. Addition of V increases the stability of the α-phase, whilst addition of Mn strongly diminishes it; the α-phase converts to γ-phase above 3% Mn. Moreover the stability of the α-phase is decreased when the pressure is increased, which is what happens in the vicinity of an interstitial. We thus think that the reduction of the stage I recovery in the concentrated **Fe**Mn alloys ($c_{Mn} \geqslant 1\%$) is likely to be related to Mn atoms in a crystallographic environment different from the α-phase of the dilute alloys.

4.2. Stage II recovery

Figure 4 shows the stage II resistivity recovery of the **Fe**Mn alloys. The stage II spectrum of the 100 ppm alloy is not much different from that of the metal. The recovery is slightly enhanced between 150 and 170 K, while the reduction observed between 180 and 200 K brings the 100 ppm spectrum close to that of purer Fe (cf figure 3 of paper I). At higher Mn concentrations, a peak develops around 165–145 K which behaves similarly to II'_{Ni}: its amplitude increases and its position shifts towards the low temperatures as the Mn concentration goes up. Moreover its amplitude is comparable to that of II'_{Ni} (and not II_{Ni}) or that of the 190 K peak observed in the **Fe**V alloys. This peak is most likely to be attributed to the free migration of mixed small poly-interstitials (such as di-interstitials) formed in stage I.

But the most striking feature of figure 4 is a large negative recovery between 160 and 200 K in the 1% and 3% alloys. This increase in the residual resistivity of the samples must be produced by a long-range migrating defect, since it is suppressed earlier in the 3% alloy than in the 1% one. We attribute it to a local phase transformation induced by mixed poly-interstitial clustering and promoted by the high pressure and high Mn concentration which exist in the mixed poly-interstitials.

The vacancy migration in stage III only partially restores the α-phase and the fractional resistivity retained at 292 K is much higher in the 1% and 3% Mn alloys than in Fe and the dilute alloys (including Fe + 1000 ppm Mn), as shown by table 4.

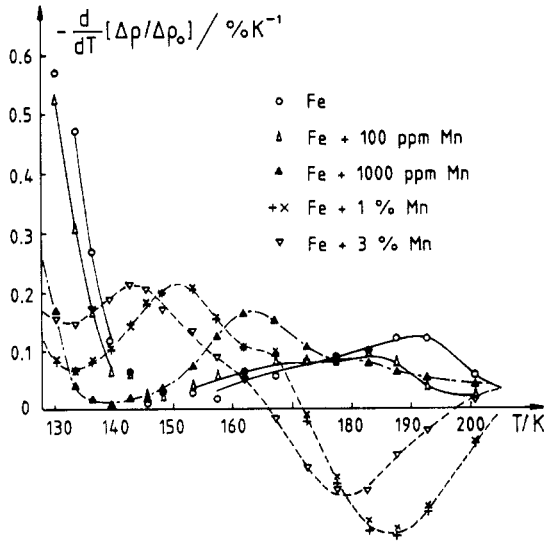

Figure 4. Same as figure 3(*a*).

Table 4. Measured percentage of the radiation-induced resistivity retained at 292 K in various Fe alloys: 100 $\Delta\rho(292\text{ K})/\Delta\rho_0$.

Solute concentration	FeMn Run No 5	FeNi Run No 6	FeNi Run No 8	FeMo Run No 7	FeV Run No 3
0	4.4	2.2	2.4	2.9–3.3	3.7
1000 ppm	4.2	0.2	—	3.8	4.2
1%	12.6–12.7	2.3–2.3	3.8	3.1	2.8
3%	28.5	3.2	4.5	5.5	0.9

That the recovery is not complete at 292 K in the 1% and 3% Mn alloys may be due to the following two points.

(i) While muon measurements (Möslang *et al* 1983) have shown that Mn atoms do not trap the single vacancies in Fe + 400 ppm Mn, the positron-annihilation measurements of Corbel (1986) have shown that Mn atoms impede the formation of large vacancy clusters: Mn atoms must retain small vacancy clusters up to at least 300 K, and thus prevent the recovery from being complete at 292 K.

(ii) Even if the mixed poly-interstitial aggregates are annealed out by the migrating vacancies, the Mn concentration may be locally high enough so that the γ-precipitates do not return to α-phase.

Before concluding, let us compare the present results with the magnetic relaxation results of Walz *et al* (1982). If we assume that the Mn atoms do trap the Fe self-interstitials, we must expect that in Fe + 1% Mn the 110 K relaxation peak due to migrating self-interstitials will be almost suppressed. Moreover, if mixed-interstitials, stable at the irradiation temperature (44 K) do form, a relaxation peak stemming from

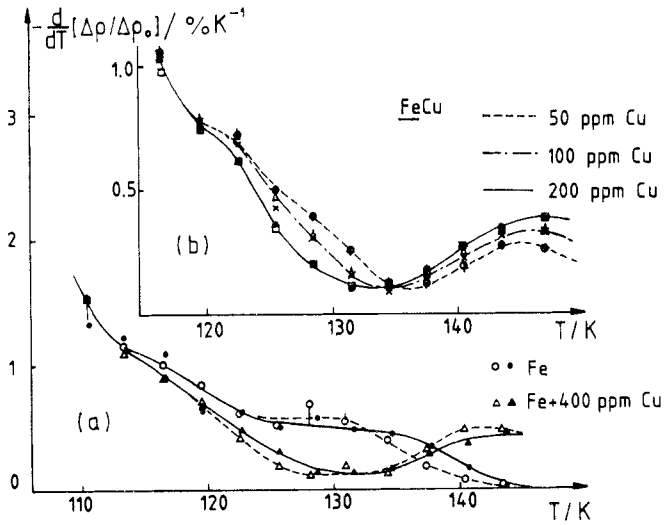

Figure 5. Differentiated isochronal recovery spectra of Fe and **Fe**Cu alloys. $\Delta t = 300$ s. $T_{irr} =$ 20–25 K, $\varphi = 6.3 \times 10^{17}$ e$^-$ cm^{-2}. (*a*) Experiment No 1: samples No 1.1 (○, ●) and 1.2 (△, ▲). Open symbols: spectra recorded after run No 1b. Full symbols: spectra recorded after run No 1c. (*b*) Experiment No 2: samples No 2.1 (○), 2.4 (+), 2.2 (△), 2.5 (×), 2.3 (□) and 2.6 (*).

these mixed-interstitials should show, in a 1% alloy, immediately after irradiation. These two points are effectively met in Fe + 1% Ni (Blythe *et al* 1984) and Fe + 0.5% Si (Walz *et al* 1982) but not in Fe + 1% Mn, except if the 110 K relaxation peak observed in this alloy is attributed to mixed interstitials Fe–Mn, migrating in the same temperature range as self-interstitials, and not only to self-interstitials. Yet this attribution which supports our model is only tentative, since we have seen that in this concentration range the situation may be more complicated than in the very dilute alloys.

5. Mixed-interstitial formation and migration in FeCu alloys

5.1. Stage I recovery

Figure 5(*a*) shows the stage I_E recovery spectrum of the alloy Fe + 400 ppm Cu, irradiated together with the **Fe**Ti alloys (see paper I); two spectra were registered after run No 1b and run No 1c, both at $T_{irr} \simeq 20$ K. Between the two runs, the sample spent a month at room temperature. No radiation-induced resistivity was left in the sample. On the contrary, from one run to the other, the initial residual resistivity of the sample, ρ_0, had decreased by about 2 nΩ cm (1.5% of ρ_0).

Figure 5(*b*) shows the stage I_E recovery spectra of the three alloys Fe + 50 ppm Cu, Fe + 100 ppm Cu and Fe + 200 ppm Cu, measured in a second experiment; two samples of each concentration were irradiated in that experiment, leaving no place for a Fe reference. No concentrated **Fe**Cu alloy was available since the solubility limit of Cu in Fe is very low: 0.5% at 700 °C, 0.2% at 650 °C (Salje and Feller-Kniepmeier 1976).

Figure 5 shows that stage I_E is gradually suppressed by increasing concentrations of Cu, indicating that the Cu atoms efficiently retain the interstitials above stage I. The

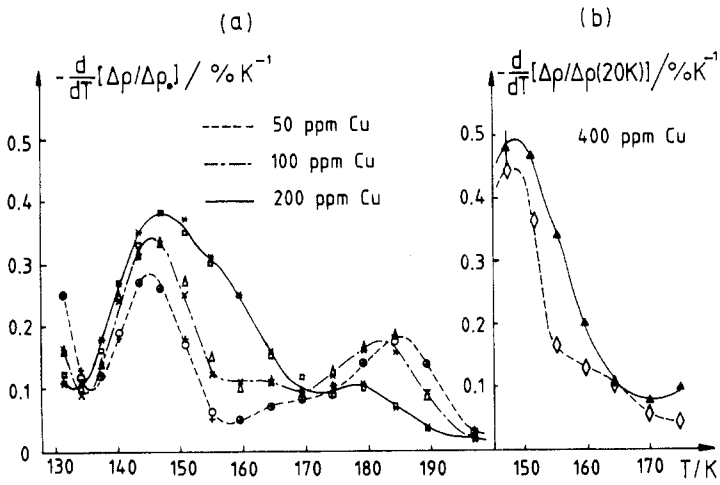

Figure 6. (*a*): Same as figure 5(*b*). (*b*) Differentiated isochronal recovery spectra of Fe + 400 ppm Cu (sample 1.2) after run No 1c: $T_{irr} \simeq 20$ K, $\varphi = 6.3 \times 10^{17}$ e$^-$ cm^{-2} (▲), and after run No 1d: $T_{irr} \simeq 120$ K, $\varphi = 16.8 \times 10^{17}$ e$^-$ cm^{-2} (◇). The data have been normalized to the measured radiation-induced resistivity, $\Delta\rho_1$ (20 K) = $\Delta\rho_0$, in the former case (▲), and to $\Delta\rho_2$ (20 K) = (16.8/6.3) $\Delta\rho_1$ (20 K) in the latter case (◇). Δt = 300 s.

fraction of radiation-induced resistivity retained at the end of stage I_E is about the same as in **Fe**Ni dilute alloys (cf table 5).

Table 5. Measured fractional resistivity retained at T_E, end of stage I_E, in **Fe**Cu and **Fe**Ni dilute alloys: $\Delta\rho(T_E)/\Delta\rho_0$ (%).

	Concentration			
Solute	50 ppm	100 ppm	200 ppm	400 ppm
Cu	17.0–17.6	18.8–19.7	20.7–21.4	21.1[1]–20.2[2]
Ni	17.5–17.9	18.0†–18.1–18.8	19.5	23.0–23.9

Footnotes: see text.

The figures pertaining to the **Fe**Ni alloys are, except for one†, taken from a previous work (Maury *et al* 1986). The figures displayed with a superscript for the 400 ppm Cu alloy were measured after the second ([1]) or third ([2]) irradiation run given to the sample. If, as suggested by figure 5(*a*), the trapping becomes less efficient from one run to the following, they may be only lower limits of $\Delta\rho(T_E)/\Delta\rho_0$.

5.2. Stage II recovery

Like in **Fe**Ni alloys, the suppression of stage I_E in **Fe**Cu alloys is followed by a recovery peak at the very beginning of stage II (figures 5 and 6). Its amplitude is comparable to that of II_{Ni} for equal solute concentrations (100 ppm), yet it is different from II_{Ni}: it is composed of at least two peaks, the first, II_{Cu}, centred around 145 K and a second one,

II'_{Cu}, centred around 165–160 K. Peak II_{Cu}, in contrast to II_{Ni}, does not shift towards the low temperatures when the solute concentration is increased but shifts slightly towards the high temperatures. This behaviour is characteristic of a detrapping peak, which is what is expected if we assume that the Fe self-interstitials have been merely trapped at the 'oversized' Cu atoms. The fractional radiation-induced resistivity retained at the end of stage II_{Cu} (157 K) in Fe + 50 ppm Cu (13.3–14.0%) is the same, within the experimental uncertainties, as that retained at 142 K in Fe (13.3 ± 0.6%), indicating that the Cu atoms do not retain the single interstitials above stage II_{Cu}.

But if we now turn to the peak II'_{Cu}, we see that it behaves quite similarly to II'_{Ni}: it shifts towards the low temperatures when the solute concentration is increased; its amplitude is comparable to that of II'_{Ni} and increases with the solute concentration more rapidly than a linear correlation, like that of II'_{Ni}. The most straightforward interpretation of peak II'_{Cu} is then to attribute it, like II'_{Ni}, to the free migration of mixed poly-interstitials. This implies that mixed interstitials Fe–Cu are formed in stage I. We are thus led to propose the following interpretation for the stage I and stage II recovery of low-temperature irradiated **Fe**Cu alloys.

Mixed-interstitials Fe–Cu are created during the self-interstitial long-range migration in stage I_E; like the mixed interstitials Fe–Mn, the mixed interstitials Fe–Cu are mobile at this temperature, but contrary to the Fe–Mn and Fe–Ni cases, they are retrapped by the remaining substitutional solute atoms and form trapped mixed interstitials or Cu–Cu interstitials stable up to the end of stage I. These trapped mixed-interstitials or hetero-interstitials Cu–Cu break up around 145 K, releasing the mixed-interstitials Fe–Cu which combine to form the mixed di-interstitials migrating around 160 K.

The attribution of II'_{Cu} to (mixed) poly-interstitials is confirmed by the fact that irradiating at a higher temperature (where the mixed interstitials Fe–Cu are mobile and not stably retrapped by the Cu atoms) and to a higher dose strongly reduces the peak II'_{Cu}, as shown by figure 6(*b*). This reduction results from the fact that the low instantaneous concentration of migrating Fe–Cu favours the nucleation of mixed-interstitial clusters on residual impurities to the detriment of the formation of mixed di-interstitials.

A third peak shows up at the end of stage II, between 170 and 200 K. This peak, whose amplitude decreases when the Cu concentration increases, most likely stems from residual impurities.

5.3. Stage III recovery

At the beginning of stage III (200 K), the retained fraction of the radiation-induced resistivity does not depend on the Cu concentration $\Delta\rho(200\text{ K})/\Delta\rho_0 = 10.5 \pm 0.5\%$.

Figure 7 displays the resistivity recovery spectra of the three alloys: Fe + 50 ppm Cu, Fe + 100 ppm Cu and Fe + 200 ppm Cu, between 190 and 290 K. On the same figure is added the recovery spectrum of an Fe sample (No 3.1) which was irradiated in the same conditions as the **Fe**Cu alloys ($T_{irr} = 20$ K, $\varphi = 7.4 \times 10^{17}$ e$^-$ cm^{-2}) and underwent the same annealing programme. Figure 7 shows that the vacancy long-range migration which takes place in the Fe sample around 230 K is hindered by the presence of copper. This agrees with the results of Möslang *et al* (1983) who show that Cu retains the single vacancies, shifting their disappearance from 200 to 210 K (their defect concentration is ten times ours).

The peak which appears below 230 K in the 200 ppm alloy (figure 7) thus cannot stem from vacancies and must be attributed to the break-up, release or migration of small

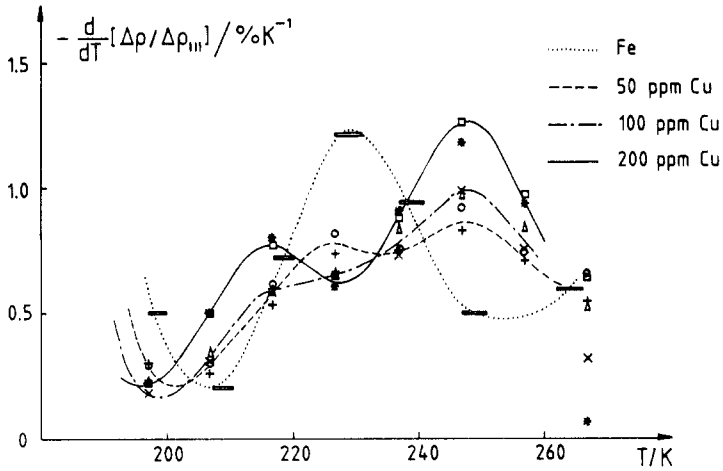

Figure 7. Differentiated isochronal recovery spectra of Fe: sample No 3.1 (▬) and **Fe**Cu alloys: samples 2.1 to 2.6, symbols as in figure 5(*b*). $\Delta t = 300$ s. The data have been normalized to the resistivity retained at the beginning of stage III (207 to 197 K depending on the alloy).

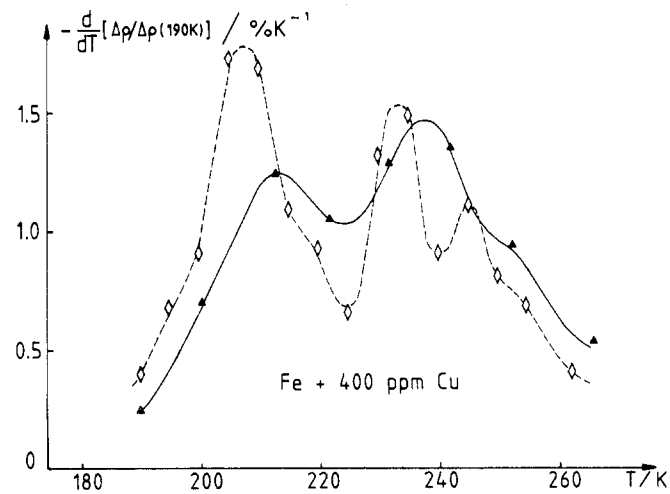

Figure 8. Differentiated isochronal recovery spectra of Fe + 400 ppm Cu (sample 1.2) after run No 1c, $T_{irr} \simeq 20$ K, $\varphi = 6.3 \times 10^{17}$ e$^-$ cm^{-2} (▲) and after run No 1d, $T_{irr} \simeq 120$ K, $\varphi = 16.8 \times 10^{17}$ e$^-$ cm^{-2} (◇). The data have been normalized to the resistivity retained at 190 K. $\Delta t = 300$ s.

interstitial clusters. Figure 8 shows that this peak, whose amplitude increases markedly as the Cu concentration goes up from 50 to 400 ppm, is enhanced when the dose is enhanced and the irradiation temperature increased. Note that the temperature shift visible in figure 8 is not significant since the annealing programme was not the same for the two spectra.

The recovery peaks which appear above 230 K can be attributed to the release of vacancies from different vacancy clusters nucleated on Cu atoms according to Corbel (1986).

As shown by table 6, the fraction of radiation-induced resistivity retained in the sample at 262 K, $\Delta\rho(262\,\mathrm{K})/\Delta\rho_0$, is a decreasing function of the Cu concentration, although the Cu atoms still trap some small vacancy clusters. After six weeks at room temperature, the residual resistivity of the 100 and 200 ppm alloys has become less than before the irradiation.

Table 6. Percentage of the radiation-induced resistivity retained at 262 and 300 K in dilute **Fe**Cu alloys.

Alloy	Fe + 50 ppm Cu	Fe + 100 ppm Cu	Fe + 200 ppm Cu
$100\ \Delta\rho(262\,\mathrm{K})/\Delta\rho_0$	5.4, 6.0	5.6, 5.6	4.8, 5.0
$100\ \Delta\rho(300\,\mathrm{K})/\Delta\rho_0$	0.0, 0.1	−0.8, −1.4	−2.2, −1.3

These resistivity measurements indicate that, like in **Fe**Ni alloys, solute bulk depletion has occurred following the low-temperature irradiation and the subsequent anneal at room temperature. The Cu agglomeration appears to be more important than the Ni one. In the alloy Fe + 200 ppm Cu, 1 to 2% of the Cu atoms seem to have been lost, corresponding to 2 to 3 ppm of 'lost' atoms. Now the initial concentration of Frenkel defects was $c_F \leqslant 25$ ppm (with $\rho_F \geqslant 2.0\,\mathrm{m\Omega\,cm}$), including the close pairs, and the concentration of vacancies at the beginning of stage III was $\simeq 2$ ppm.

Similar figures were obtained with the Fe + 400 ppm Cu alloy. The residual resistivity loss was 1.9, 2.0 and 1.7 nΩ cm after three successive irradiation runs at 20 K and about the same defect concentration, $c_F \simeq 25$ ppm. This corresponds to about 6 ppm of Cu atoms 'lost' after each irradiation. It seems hardly possible that vacancies at concentrations as low as a few ppm may be able to significantly agglomerate the Cu atoms in these very dilute alloys where solute clustering requires a large number of jumps. We thus think that the high efficiency of the Cu clustering after low-temperature irradiation and room-temperature annealing must principally result from the formation and migration of mixed-interstitial clusters. That solute agglomeration is more important in **Fe**Cu alloys than in **Fe**Ni alloys may result from one or several of the following points.

(i) Two Cu atoms in a Cu–Cu interstitial or trapped mixed-interstitial have, according to our model, a small positive binding energy; this is not the case for two Ni atoms.

(ii) Mixed poly-interstitials $(M\text{–}Fe)_n$ of the same size, including the single interstitial ($n = 1$), are more mobile in the Cu case than in the Ni case, which allows the formation of larger clusters before vacancy migration sets in.

(iii) Small mixed-interstitial clusters may be more tightly bound in the Cu case than in the Ni case.

(iv) Cu may affect vacancy clustering differently than Ni, and the final agglomeration state of the solute atoms at the end of stage III may depend on the clustering of vacancies in stage III: a poly-vacancy v_n arriving on a mixed poly-interstitial will leave n gathered solute atoms, while the arrival of a monovacancy may produce a smaller unstable or mobile cluster and finally results in solute dispersion.

Table 7.

Solute	Ni	Mn	Cu
Volume size factor (%):			
of the solute in Fe	+4.7	+4.9	+17.5
of Fe in the solute	+10.6	−3.7	+4.6
Pauling metallic radius (Å)	1.24	1.27	1.28

6. Summary

Let us briefly review the main points acquired from the present work.

(i) Bound mixed interstitials are formed with Ni, Mn and Cu atoms, although the size effect of Mn and Cu in Fe is slightly positive, as shown by table 7.

This positive size effect cannot account for the formation of mixed interstitials but is small enough not to forbid it as in the case of V, Mo, Au or Ti. To explain that the mixed interstitials Fe–Ni, Fe–Mn and Fe–Cu are effectively bound, the magnetic properties of the defect have to be taken into account. We expect the magnetic properties of the core of the defect to be the decisive parameter for the mixed-interstitial binding.

(ii) Mixed interstitials Fe–Mn and Fe–Cu are as mobile as (or even more mobile than) Fe–Fe self-interstitials, while mixed-interstitials Fe–Ni are stable up to 20 K higher. The former case leads to a somewhat paradoxical situation where mixed-interstitials are both more stable (they form more easily) and less stable (they migrate more easily) than self-interstitials. Now we expect the defect mobility to depend not only on the magnetic properties of the core of the defect but also on the magnetic properties of its surroundings. We note that while the magnetic moment per solute atom is similar for Ni and Mn (1.4 and 1.0 μ_B as compared to 2.2 μ_B for Fe), the total host moment perturbation is positive for Ni and negative for Mn (Stearns 1976).

(iii) Solute–solute split interstitials (two solute atoms sharing a lattice site) or mixed interstitials trapped at a solute atom at the stage I_E temperature are slightly bound in the case of Cu while not in the case of Mn (nor in the case of Ni above stage II_{Ni}). This may be related to the interaction potential between two solute atoms, which is found to be repulsive for two Mn atoms closer than third-nearst neighbours (Pierron and Cadeville 1982), impeding Mn precipitation in **Fe**Mn alloys, while Cu precipitates at very low concentrations in **Fe**Cu alloys.

(iv) Small mixed poly-interstitials form and migrate without dissociating in stage II of the three alloys **Fe**Ni, **Fe**Mn and **Fe**Cu, leading to solute gathering in small interstitial clusters. There exists a number of *a priori* possible configurations for mixed di-interstitials and still more possible migration (as well as re-orientation) mechanisms. Several of these possibilities may effectively be encountered with slightly different formation and migration energies. Resistivity measurements are unable to distinguish between all of them.

(v) In **Fe**Ni and **Fe**Cu alloys and probably in the **Fe**Mn most dilute alloys, irradiated at low-temperature, mixed-interstitial clustering significantly contribute to solute bulk depletion.

(vi) In **Fe**Mn alloys, with a manganese concentration in the per cent range, mixed-interstitial clustering leads to γ-precipitation which is not entirely annealed out at the end of stage III or room temperature.

References

Arajs S, Schwerer F C and Fisher R M 1969 *Phys. Status Solidi* **33** 731
Blythe H J, Walz F and Kronmüller H 1982 *Phys. Status Solidi* a **69** 347
—— 1984 *Phys. Status Solidi* a **81** 227
Börner C, Bohn H G and Robrock K-H 1987 *Mater. Sci. Forum* **15/18** 617
Campbell I A, Fert A and Pomeroy A R 1967 *Phil. Mag.* **15** 977
Corbel C 1986 *Rapport CEA-R-5334*
Dorleijn J W F and Miedena A R 1977 *J. Phys. F: Met. Phys.* **7** L23
Fert A and Campbell I A 1976 *J. Phys. F: Met. Phys.* **6** 849
Kaufman L and Ringwood A E 1961 *Acta Met.* **9** 941
King H W 1966 *J. Mater. Sci.* **1** 79
Little E A 1984 *Dimensional Stability and Mechanical Behaviour of Irradiated Metals and Alloys* (London: Brit. Nucl. Energy Soc.)
Maury F, Lucasson A, Lucasson P and Dimitrov C 1988 *J. Phys. F: Met. Phys.* **18** 657
Maury F, Lucasson A, Lucasson P, Faudot F and Bigot J 1987 *J. Phys. F: Met. Phys.* **17** 1143
Maury F, Lucasson A, Lucasson P, Loreaux Y and moser P 1986 *J. Phys. F: Met. Phys.* **16** 523
Maury F, Lucasson A, Lucasson P, Moser P and Faudot F 1990 *J. Phys.: Condens. Matter* **2** 9269–90
Möslang A, Albert E, Recknagel E and Weidinger A 1983 *Hyperfine Interact.* **15/16** 409
Pierron V and Cadeville M C 1982 *J. Phys. F: Met. Phys.* **12** 549
Robrock K-H 1987 *Mater. Sci. Forum* **15/18** 537
Salje G and Feller-Kniepmeier 1977 *J. Appl. Phys.* **48** 1833
Stearns M B 1976 *Phys. Rev.* B **13** 1183
Vigier P 1966 *Thèse Université Grenoble*
Vigier P and Moser P 1966 *C.R. Acad. Sci., Paris* **262** 327
Walz F, Blythe H J and Dworschak F 1982 *Phys. Status Solidi* a **75** 235